

Verification Testing of Wind Speed Measurements from 2D Sonic Anemometers

Adam Havner, Rachael V. Coquilla, and John Obermeier
Otech Engineering, Inc., Davis, CA 95618 USA

ABSTRACT: Sonic anemometers are used to measure wind speed in 1, 2, or 3 dimensional flows by relating the change in sound waves (Doppler shift) to the magnitude of the passing wind. For sonic sensors configured to measure 2D or 3D flows, it is also possible to determine the wind direction. Because of the ability to characterize such flows, sonic anemometers are essential instruments for atmospheric turbulence. Available standards for the performance testing of sonic anemometers are ASTM D 6011-96 and ISO 16622, which involves a rigorous test program that evaluates the inherent three-dimensional characteristic of sonic anemometers. For sonic sensors used in research applications, where it may be necessary to map complex flows at high resolution, such detailed test procedures for the sonic instrument may be necessary. However, some of the most common industry applications for sonic anemometers generally only require a certain level of uncertainty in two dimensional wind speed and direction measurements such as on weather stations, airports, oceanic buoys, nuclear power plants, wind plants, and many others. Thus, a more practical test protocol, extracted from published test standards, may be applicable for verifying sonic anemometer wind measurements. Such a test protocol may also be designed to the specific range of wind speeds critical to certain industries. Based on the guidelines provided in ASTM D 6011-96 and ISO 16622 and a similar test method used in the acceptance testing for the sonic sensor model employed for the Automated Surface Observing System (ASOS) of the United States National Weather Service (NWS), this presentation proposes a wind speed verification process for 2D sonic anemometers.

A. Introduction

Wind measurement from sonic anemometers is related to the change in the propagation of sound waves between a sound transmitter (i.e., speaker) and a receiver. Two standards that define procedures for sonic anemometer testing are ASTM D 6011-96 and ISO 16622. These standards describe the initial calibration for a sonic anemometer in a zero-wind chamber, which involves the measurement of the acoustic pathlength and transient times between the transmitter and receiver. However, there are also several factors that affect the sound measurement of a sonic anemometer. Sonic sensors are particularly sensitive to the local density and to the angle of the incoming wind. To fully gain understanding of the sensor's performance, the response of a sonic sensor is further evaluated through various temperature and pressure environments in the zero-wind chamber. This evaluation defines the corrections to the sonic wind speed reading due to changes in local density. In addition, objects, positioned upwind of the path between the sound transmitter and receiver, are also known to disturb the sound wave propagation. Standards also recommend that the sensor's response be evaluated when subjected to various angles of incoming flow in a wind tunnel. One of the most difficult challenges with sonic sensors is the three-dimensional sensitivity, in which the horizontal wind speed reading is greatly affected by vertical or off-axis flow. In general, test protocols defined by standards are designed for evaluating prototype sensors or for sonic sensors deployed for critical research applications. For sonic sensors deployed in meteorological stations and weather monitoring stations, a simplified version of the ISO 16622 test protocol may be all that is necessary for the required wind measurement precision. This proposed wind speed verification-type protocol is similar to the methods performed for the acceptance testing of the sonic sensor model employed for the Automated Surface Observing System (ASOS) of the United States National Weather Service (NWS).

B. Review of Sonic Anemometer Test Standards

Test protocols in this study were based on standards used for general meteorology applications. Two, in particular, are ASTM D 6011-96: "Standard test method for determining the performance of a sonic anemometer/thermometer" and ISO 16622: "Meteorology – Sonic anemometers/thermometers – Acceptance test methods for mean wind measurements".

ASTM D 6011-96 is a sonic anemometer performance test standard originally released in 1996 and its current version released in 2008. This standard is intended to assist wind instrument manufacturers in the design and development of a sonic anemometer deployed for general meteorological applications. It is also used as a guide for test facilities and end-users for evaluating the performance of a sonic anemometer used in specific wind measurement applications. Procedures in ASTM D 6011-96 include measurements of the: 1) acoustic pathlength, 2) system delay, 3) system delay mismatch, 4) thermal stability range, 5) velocity resolution, 6) shadow correction, 7) velocity calibration range, and 8) the acceptance angle. The first five tests are done in a zero-wind chamber which defines the initial calibration transfer characteristics of the instrument. The following three measurements, shadow correction, velocity calibration range, and acceptance angle, define the necessary corrections to the initial calibration transfer characteristics and are determined through the response of the sonic anemometer in a controlled wind tunnel facility having requirements defined in Table 1 below.

Table 1: Wind tunnel requirements for ASTM D 6011-96 sonic sensor testing.

<i>Wind Tunnel Characteristic</i>	<i>Minimum Requirement</i>
Blockage	Anemometer front area is less than 5% of the test section cross-section area
Wind Speed Capability	Must be capable of reaching speeds up to at least 50% of the application range and must maintain speed within +/- 0.2 m/s. Wind tunnel speeds from 1.0 to 10 m/s be maintained at +/- 0.1 m/s or better.
Flow Uniformity	Flow profile in the test section must be constant to within 1%
Turbulence	Must be less than 1% in the test section
Air Density Uniformity	Density profile in test section must be less than 3% difference
Wind Speed Reading	Maintain a relative accuracy of 0.1 m/s to its traceable source

Shadow correction accounts for the effect of the three-dimensional flow inherently sensed by sonic anemometers. This is determined by measuring the sonic anemometer response at multiple orientations around the horizontal and vertical plane with respect to the incoming controlled wind tunnel flow. An apparatus used to rotate the anemometer around the horizontal and vertical plane requires an angular alignment resolution of 0.5°. Shadow correction creates a calibration "look-up" table or correction function, which may be used to adjust the sonic anemometer wind speed output when subjected to the particular off-angle position from the incoming flow. The following steps summarize the procedures in ASTM D 6011-96 to conduct shadow correction performance tests on sonic anemometers in a wind tunnel facility. Overall, the ASTM procedures involve a total of 252 test settings.

Step 1: With the sensor positioned at zero angle of attack, select a low wind speed (about 2 m/s or lower) to test for orientations +/- 60 degrees around its vertical axis at 10 degree increments. Repeat this procedure for a mid-range speed (about 5 to 6 m/s) and then for a high wind speed (about 10 m/s or greater).

Step 2: Repeat Step 1 for angles of attack at 5 degree increments starting with the sensor tilted 15 degree into the wind to 15 degree tilted away from the wind.

An international standard for conducting sonic anemometer performance testing is ISO 16622, which was released in September 2002. The goal of this standard is similar to that of ASTM D 6011-96 in that it provides the procedures that capture the three-dimensional response of a sonic anemometer. ISO 16622 defines the following four test methods:

- 1) Zero wind chamber test, which determines the zero wind offset for the instrument.
- 2) Wind tunnel test, which characterizes the deviation of the wind speed due to the angle of the incoming flow (i.e. shadow correction testing)
- 3) Pressure chamber test, which defines the operational air density range for the instrument.
- 4) Field test, which evaluates the sensor under possible adverse environmental conditions difficult to simulate in a laboratory.

ISO 16622 requirements for a wind tunnel facility are also similar to that in ASTM D 6011-96. However, ISO 16622 additionally suggests that the wind tunnel be capable of producing wind speeds that cover the full application range of the sonic anemometer to be calibrated. Each steady setting of the wind speed must be maintained to within ± 0.2 m/s, preferably ± 0.1 m/s. For angle testing, the rotating fixture must have a 1° angular resolution and $\pm 0.5^\circ$ repeatability. The wind tunnel test protocol in ISO 16622 is defined as follows and totals to 1,140 test settings:

Step 1: With the sensor positioned at zero angle of attack, select a low wind speed (about 10% of the maximum test speed) to test for orientation ± 360 degrees around its vertical axis at 5 degree increments. Repeat step for 18%, 32%, 56%, and 100% of the maximum test speed.

Step 2: With the sensor positioned vertically at zero angle of attack and rotated at the worst case orientation (where the sensor reading is most disturbed by support structures), perform tests at 1%, 1.7%, 2.8%, 4.6%, 7.7%, 13%, 21%, 36%, 60%, and 100% of the maximum test speed. If such a wind speed range is not feasible for the wind tunnel lab, perform tests at 2%, 3%, 5%, 7%, 11%, 18%, 27%, 42%, 65%, and 100% of the maximum test speed. Repeat step for the best case orientation (where the sensor is least disturbed by support structures).

Step 3: Repeat Steps 1 and 2 with the sensor tilted 15 degrees into the wind and then tilted 15 degrees away from the wind.

C. Sonic Sensor Test Setup

For this study, sonic sensors shown in Figure 1 were tested in the Otech Wind Tunnel Test Facility, WT3A, located in Davis, California. The Gill WindObserver II, Gill WindSonic, and R.M. Young 85000 are new sensors loaned to Otech by the respective manufacturers, while the Met One 50.5 is a used sensor previously deployed for a short-term graduate field research work by students at University of California, Davis. Results in this study may be influenced by the condition of the sensor. A comparison of results based on the sensor condition was, however, not a part of this study, but may be performed in the future.



Figure 1: Sonic anemometer models tested in Otech Wind Tunnel, WT3A.

From Figure 1, the value for solid blockage represents the presence of the anemometer in the wind tunnel flow. This is calculated by taking the projected frontal area of the sonic sensor and its mount and dividing by the cross-sectional test section area of WT3A. Published standards recommend that the solid blockage be less than 5%. Sonic sensors tested in Otech WT3A for this study are acceptable to this requirement, except for the R.M. Young 85000, which has a solid blockage of 5.7%. Thus, for this sensor, standards also recommend to have a blockage correction applied. Based on a comparison of the results, blockage corrections were not applied to the test data of all the sensors. Later in the discussion of results, it was found that there is only minimal effect from blockage. In general, further study is needed in understanding the effect of blockage to the wind tunnel flow.

Otech Engineering, Inc. is an ISO/IEC 17025:2005 accredited laboratory and operates three suction-type (Eiffel-type) wind tunnels that are housed in separate laboratory rooms. All of the wind tunnels were designed with a closed test section of similar size 61.0 cm crosswind width x 61.0 cm height x 121.9 cm downwind length. For this study, tests were performed in Otech Wind Tunnel, WT3A, which is driven by a 30 hp (22 kW) fan motor that generates winds up to 45 m/s. Wind tunnels at Otech are also equipped with National Instruments LabVIEW data acquisition software and hardware that allows for near-real time, simultaneous data collection from all instruments installed, including the signal output from the anemometer undergoing calibration testing. All instruments installed are traceable to NIST.



Figure 2: Otech Engineering Wind Tunnel Laboratory, WT3A: (a) Overall view, (b) Close-up view of test section, and (c) Sample LabVIEW front panel display.

Reference wind speed in the wind tunnel test section is measured using a Pitot-static tube system where the sensing tips of four (4) Pitot-static tubes are positioned at the entrance of the test section. Dynamic and static pressure inputs from the four Pitot-static tubes are ported to a single MKS Barotron type differential pressure transducer as shown in Figure 3 below.

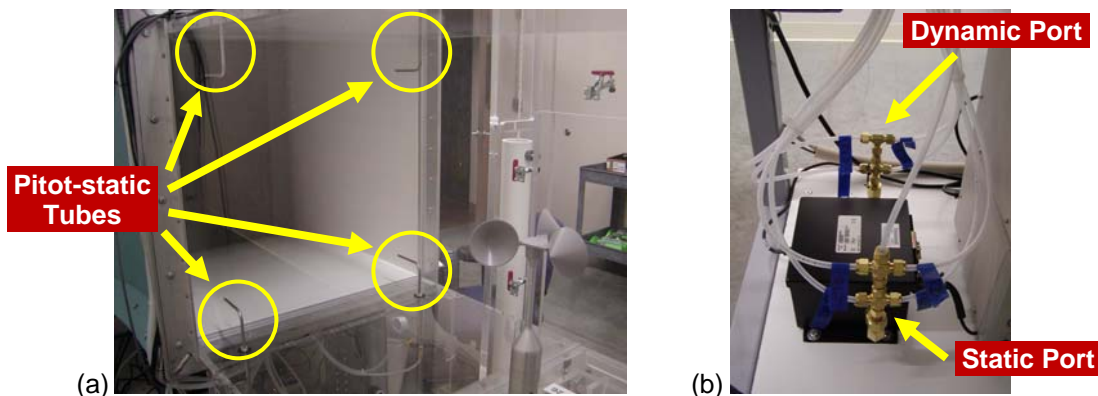


Figure 3: (a) Otech Wind Tunnel WT3A Pitot-static tube system installed in test section and (b) ported to an MKS Barotron differential pressure transducer.

Local conditions in the test section (i.e., ambient pressure, temperature, and relative humidity) are simultaneously measured in order to determine the corresponding local density used to calculate the reference wind speed. Test section ambient pressure is measured through the static ports of the Pitot-static tubes using a Setra Model 270 barometer (Figure 4a). Temperature and relative humidity is sensed by an Omega Model HX 94V probe inserted inside the test section (Figure 4b).

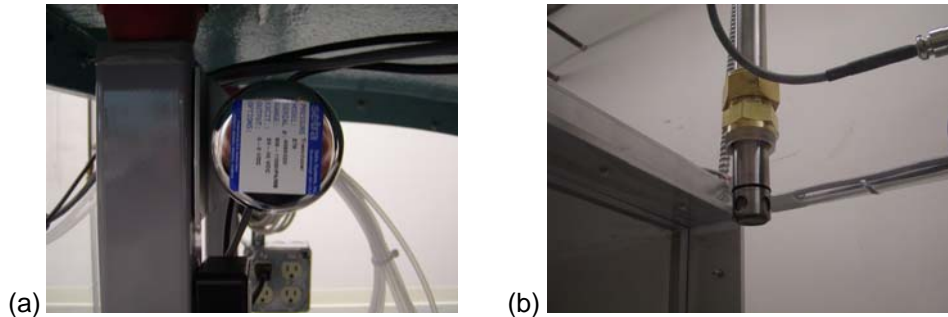


Figure 4: (a) Setra Model 270 Barometer and (b) Omega Model HX 94V Temperature and Relative Humidity probe installed in Otech Wind Tunnel WT3A.

D. Sonic Sensor Verification Test Protocol

Sonic sensor test procedures in this paper are based on methods suggested in ISO 16622 and are similar to the acceptance tests used for the sonic sensor employed for ASOS. In ISO 16622, tests were designed using the first two steps of wind tunnel procedures previously defined in Part B of this paper. For tests in this project, modifications were made in the wind speed settings to meet the common range in the wind energy industry. Therefore, sonic sensor verification tests were designed as follows:

- 1) **Direction Test:** collect sonic wind speed measurements at five (5) wind tunnel speed settings (4, 10, 16, 26, and 36 m/s) and at direction orientations of five (5) degree increments around the entire sensor.
- 2) **Verification Test:** collect wind speed readings at the best and worst orientations for a test speed range of 4 to 26 m/s at 2 m/s increments.

Out of the two methods above, the most rigorous and lengthy is the Direction Test. This paper investigates whether the much simpler Verification Test can provide roughly similar results comparable to those presented in the more extensive Direction Test. One of the areas of evaluation is in terms of expanded test uncertainty.

E. Sonic Sensor Test Uncertainty

Test uncertainty provides a quantitative method of understanding the degree of error in a measurement or defines the range in which that measurement could be. Since the sonic sensor verification tests involves the relationship between the reference wind speed reading and the sonic sensor output, an expanded test uncertainty, U_{ver} , is evaluated based on the propagation of uncertainties accumulated in the following three areas and is defined according to the following Equation (1).

- 1) U_V , uncertainty in the reference wind speed from the wind tunnel Pitot-static tube system
- 2) U_{sonic} , uncertainty in the wind speed output from the sonic sensor undergoing testing
- 3) U_D , standard uncertainty based on deviations between the reference wind speed and the sonic sensor wind speed

$$U_{ver} = \sqrt{(U_V)^2 + (U_{sonic})^2 + (U_D)^2} \quad \text{Eq. (1)}$$

IEC 61400-12-1 specifies that anemometer testing is performed using a controlled wind tunnel test facility that incorporates a Pitot-static tube system to measure the steady reference wind speed. This standard also provides a method of uncertainty calculation for this technique of wind speed. Since the Otech Wind Tunnel WT3A is installed with a Pitot-static tube system, uncertainty analysis in the reference wind speed is based on the guidelines from IEC 61400-12-1 where details in the method is based on the approach offered by Coleman and Steele (2009)⁽⁶⁾. Thus, uncertainty analysis initiates with the key data reduction equation for the calculation of the wind speed. With a Pitot-static tube system, wind speed, V , is calculated using the following base equation according to IEC 61400-12-1.

$$V = k_b \sqrt{\frac{2k_c \Delta p}{C_h \rho}} \quad \text{Eq. (2)}$$

Here, Δp is the differential pressure reading from the Pitot-static tube, C_h is the Pitot-static tube head coefficient, ρ is the density, k_c is the wind tunnel calibration factor, and k_b is the blockage correction. In more detail, the density can be defined in terms of the ambient pressure, P , the ambient temperature, T , the relative humidity, ϕ , vapor pressure, P_w , the gas constant for air, R_{air} , and the gas constant for water, R_w , as defined in the following Equation (3), followed by the definitions for the vapor pressure and gas constants, where R is the universal gas constant. M_{air} and M_w are the molecular weights for air and water.

$$\rho = \frac{1}{T} \left[\frac{P}{R_{air}} - 0.01\phi P_w \left(\frac{1}{R_{air}} - \frac{1}{R_w} \right) \right] \quad \text{Eq. (3)}$$

$$P_w = 0.0000205 \exp(0.0631846T) \quad \text{Eq. (4)}$$

$$R_{air} = \frac{R}{M_{air}} \quad \text{Eq. (5)}$$

$$R_w = \frac{R}{M_w} \quad \text{Eq. (6)}$$

By substituting Equations (3), (4), (5), and (6) into Equation (2), an expanded wind speed equation can be defined as shown in Equation (7). This form of the wind speed equation allows a more direct identification of the variables that are most sensitive to the calculation. Thus, it is considered the key data reduction equation (DRE) for uncertainty analysis.

$$V = k_b \sqrt{\frac{2k_c \Delta p R T}{C_h \left[P M_{air} - 2.05 \times 10^{-7} \phi e^{0.0631846T} (M_{air} - M_w) \right]}} \quad \text{Eq. (7)}$$

An initial evaluation of Equation (7) identified that the independent variables, or terms with exact values as defined in NIST, are found to be M_{air} and M_w . Since independent variables have no systematic or random errors, further sensitivity analysis are not required. Dependent variables are measured or pre-calculated parameters which do require further analysis. From Equation (7), uncertainty in the wind speed measured by a Pitot-static tube system is a function of the dependent variables k_b (blockage correction), k_c (wind tunnel correction), C_h (Pitot-static tube correction), R (universal gas constant), P (ambient pressure), T (ambient temperature), Δp (Pitot-static tube differential pressure), and ϕ (relative humidity).

Uncertainty in the reference wind speed is defined as the sum of the squares of the systematic or bias error contributions and of the random or precision error contributions:

$$U_V = \sqrt{B_V^2 + (tS_V)^2} \quad \text{Eq. (8)}$$

Here, B_V represents the propagation of systematic or bias error contributions to the wind speed measurement and is a function of all the dependent variables found in Equation (7). These types of errors are typically considered Type B⁽⁵⁾. The propagation of systematic or bias errors is defined in:

$$B_V = \sqrt{\left(\frac{\delta V}{\delta k_b} B_{k_b} \right)^2 + \left(\frac{\delta V}{\delta k_c} B_{k_c} \right)^2 + \left(\frac{\delta V}{\delta C_h} B_{C_h} \right)^2 + \left(\frac{\delta V}{\delta R} B_R \right)^2 + \left(\frac{\delta V}{\delta P} B_P \right)^2 + \left(\frac{\delta V}{\delta T} B_T \right)^2 + \left(\frac{\delta V}{\delta \Delta p} B_{\Delta p} \right)^2 + \left(\frac{\delta V}{\delta \phi} B_\phi \right)^2} \quad \text{Eq. (9)}$$

In Equation (9), terms indicated with “B” are the bias errors from each of the dependent variables, identified by the subscript. For the measured variables, P , T , Δp , and ϕ , bias errors can be found from data acquisition, signal conditioning, and instrument performance such as linearity or accuracy. For the assigned or property variables, k_b , k_c , C_h , and R , “fossilized” errors are generally applied, representing both the random and systematic errors in the determination of such variables.

From Equation (8), S_V signifies the propagation of random or precision error contributions which originate from the dependent measured variables, P , T , Δp , and ϕ , and are typically considered Type A⁽⁵⁾. The value of t for 95% confidence at ∞ degrees of freedom is 1.96⁽⁶⁾. Propagation of random errors is defined as according to the following Equation (10), where terms indicated with “S” are the random errors and are essentially the standard deviations of corresponding measured variables.

$$S_V = \sqrt{\left(\frac{\delta V}{\delta P} S_P\right)^2 + \left(\frac{\delta V}{\delta T} S_T\right)^2 + \left(\frac{\delta V}{\delta \Delta p} S_{\Delta p}\right)^2 + \left(\frac{\delta V}{\delta \phi} S_\phi\right)^2} \quad \text{Eq. (10)}$$

For both Equations (9) and (10), the partial differentials at the front of each term are the corresponding sensitivity coefficients of each dependent variable. These partial differentials are derived from the expanded wind speed term, Equation (7), and are listed in the following Table 1. Note that by substituting the expanded wind speed term into each of the partial differentials, the sensitivity coefficient equations can be further simplified to match similar terms given in the sample uncertainty analysis provided in IEC 61400-12-1. Although there are some differences in the sensitivity analyses, the final accounting of the measurement errors is essentially similar. One specific variable that differs from IEC 61400-12-1 is the analysis to the barometer sensitivity. From this method, the barometer sensitivity contributes a positive effect in the uncertainty; whereas in IEC 61400-12-1, this is a negative effect.

Table 1: Sensitivity coefficients for each dependent variable in the wind speed uncertainty.

Variable	Sensitivity Coefficient Equation	Equation
Blockage Coefficient	$\frac{\delta V}{\delta k_b} = \frac{1}{C_h} \sqrt{\frac{2k_c \Delta p R T}{PM_{air} - 2.05 \times 10^{-7} \phi e^{0.0631846T} (M_{air} - M_w)}} = \frac{V}{k_b}$	Eq. (11)
Pitot-static Tube Head Coefficient	$\frac{\delta V}{\delta C_h} = -\frac{1}{2} \frac{k_b}{C_h^{3/2}} \sqrt{\frac{2k_c \Delta p R T}{PM_{air} - 2.05 \times 10^{-7} \phi e^{0.0631846T} (M_{air} - M_w)}} = -\frac{1}{2} \frac{V}{C_h}$	Eq. (12)
Universal Gas Constant	$\frac{\delta V}{\delta R} = \frac{1}{2} k_b \sqrt{\frac{2k_c \Delta p T}{RC_h [PM_{air} - 2.05 \times 10^{-7} \phi e^{0.0631846T} (M_{air} - M_w)]}} = \frac{1}{2} \frac{V}{R}$	Eq. (13)
Ambient Pressure	$\frac{\delta V}{\delta P} = -\frac{1}{2} \frac{k_b M_{air}}{[PM_{air} - 2.05 \times 10^{-7} \phi e^{0.0631846T} (M_{air} - M_w)]^{3/2}} \sqrt{\frac{2k_c \Delta p R T}{C_h}}$ $= -\frac{1}{2} \frac{VM_{air}}{PM_{air} - 2.05 \times 10^{-7} \phi e^{0.0631846T} (M_{air} - M_w)}$	Eq. (14)
Ambient Temperature	$\frac{\delta V}{\delta T} = k_b \sqrt{\frac{2k_c \Delta p R}{C_h}} \frac{0.5(T)^{-1/2} [PM_{air} - 2.05 \times 10^{-7} \phi e^{0.0631846T} (M_{air} - M_w)]^{1/2} - 0.5 [PM_{air} - 2.05 \times 10^{-7} \phi e^{0.0631846T} (M_{air} - M_w)]^{-1/2} (T)^{1/2}}{PM_{air} - 2.05 \times 10^{-7} \phi e^{0.0631846T} (M_{air} - M_w)}$ $= \frac{1}{2} V \left[\frac{1}{T} + \frac{1.295 \times 10^{-8} \phi e^{0.0631846T} (M_{air} - M_w)}{PM_{air} - 2.05 \times 10^{-7} \phi e^{0.0631846T} (M_{air} - M_w)} \right]$	Eq. (15)

Variable	Sensitivity Coefficient Equation	Equation
Differential Pressure	$\frac{\delta V}{\delta \Delta p} = \frac{1}{2} k_b \sqrt{\frac{2k_c RT}{\Delta p C_h [PM_{air} - 2.05 \times 10^{-7} \phi e^{0.0631846T} (M_{air} - M_w)]}} = \frac{1}{2} \frac{V}{\Delta p}$	Eq. (16)
Relative Humidity	$\begin{aligned} \frac{\delta V}{\delta \phi} &= -\frac{1}{2} \frac{k_b [-2.05 \times 10^{-7} \phi e^{0.0631846T} (M_{air} - M_w)]}{[PM_{air} - 2.05 \times 10^{-7} \phi e^{0.0631846T} (M_{air} - M_w)]^{3/2}} \sqrt{\frac{2k_c \Delta p RT}{C_h}} \\ &= \frac{1}{2} \frac{V [-2.05 \times 10^{-7} \phi e^{0.0631846T} (M_{air} - M_w)]}{PM_{air} - 2.05 \times 10^{-7} \phi e^{0.0631846T} (M_{air} - M_w)} \end{aligned}$	Eq. (17)

Overall, the dominant variables in a controlled test that affect the uncertainty in the wind speed originate primarily from the contribution of bias or systematic errors (Type B). Smaller random or precision errors (Type A), driven by lower standard deviations in the readings, imply that readings at each test speed are stable. According to the sensitivity analysis, it is also critical to choose temperature and differential pressure instruments of the appropriate accuracy and resolution for calibration testing. For the Otech Wind Tunnel WT3A, the average uncertainty in the reference speed is typically about 0.47%.

A second contribution to the uncertainty in the sonic sensor verification test comes from the sonic anemometer wind speed measurement. This uncertainty is identified in this paper as U_{sonic} and is defined in Equation (18), where B_{sonic} and S_{sonic} are the propagation of bias and random errors, respectively.

$$U_{sonic} = \sqrt{B_{sonic}^2 + (tS_{sonic})^2} \quad \text{Eq. (18)}$$

Bias or systematic errors in the sonic sensor output are primarily from the data acquisition system. Random or precision errors are determined from the standard deviation of sonic sensor output reading during the duration of the data collection. Here, the value of t for 95% confidence at ∞ degrees of freedom is 1.96⁽⁶⁾. In general, the uncertainty in the sonic sensor output signal signifies the degree of stability in the reading when subjected to steady wind flow conditions.

To evaluate the relationship between the wind tunnel reference wind speed and the sonic sensor output wind speed, wind differences were calculated at each test point. As a final contribution to the uncertainty in the sonic sensor tests, an uncertainty due to this relationship, U_D , was defined based on the percent differences calculated at each test point. This generally represents the bias associated in relating the sensor output to a NIST traceable wind speed measurement system. In this case, the percent difference is calculated according to the following Equation (19), where V is the reference wind speed, as defined from Equation (7), and V_{sonic} is the wind speed measurement from the sonic sensor.

$$U_D = \frac{V - V_{sonic}}{V} \quad \text{Eq. (19)}$$

Uncertainty methods described in this section were applied to both the sonic sensor Direction Tests and Verification Tests. For the Direction Tests, an expanded uncertainty using Equation (1) was calculated for each direction orientation test setting. The overall uncertainty in the Direction Tests was determined by taking the average of the expanded uncertainties at each direction orientation setting. From the Verification Tests, expanded uncertainty was evaluated at each test speed setting. Overall uncertainty in the Verification Tests was determined by averaging the expanded uncertainties at each test speed from both the best and worst direction orientations. Included in the overall uncertainty in the Verification Tests is also the standard deviation in the wind speed differences at each test speed, which applies as an additional accumulation of bias error. The goal here is to show that both types of tests may show a common representation for the performance of a sonic sensor based on the similarities in uncertainty. In general, uncertainty defines the range in which a measured value could fall.

F. Results from Direction Tests

With data from the Direction Tests, comparisons were made between the wind speed reading from the Pitot-static tube system and from the sonic sensor undergoing the test. To ensure an acceptable rotational position of the sonic sensor, the wind direction output from the sensor was compared to a mechanical position reading identified by polar rotation marks on the test tray as shown in Figure 5 below. A close-up view of the polar rotation marks is shown in the following Figure 6.

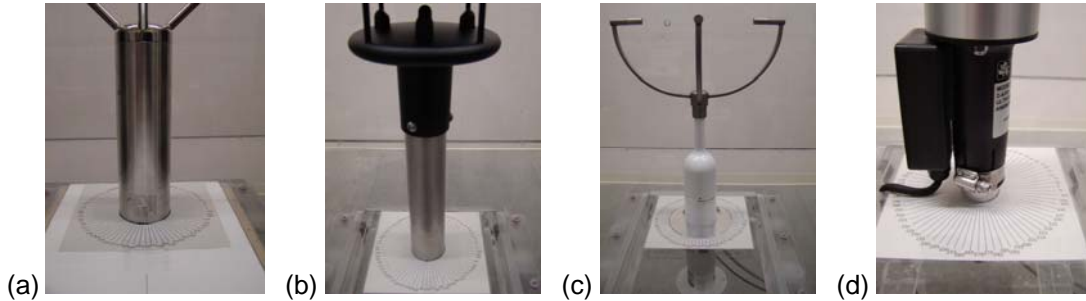


Figure 5: Setup of sonic sensor rotation mechanical positioning for the (a) Gill WindObserver II, (b) Gill WindSonic, (c) Met One 50.5, and (d) R.M. Young 85000.

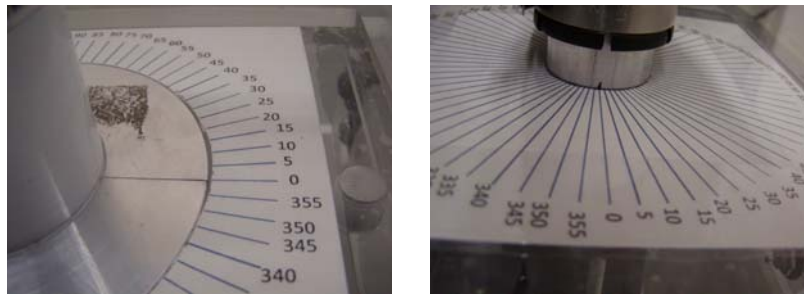


Figure 6: Close-up view of polar rotation marks on sonic sensor test trays.

Figures 7 to 10 below are plots of percent wind direction difference between the mechanical positioning and the sonic sensor wind direction reading as a function of the sonic sensor wind direction reading. These results show that the highest wind direction deviations were measured with the R.M. Young 85000 at the 160 to 300 degree wind direction readings. These larger deviations in the readings may either be an indication of flow disturbance affecting the sensor wind direction reading or errors in the manual mechanical positioning, which at best can be within +/- 0.2% or +/- 1 degree. Overall, wind direction output from the sonic sensors maintained an average difference of less than 0.5% from the mechanical setting and revealed that the wind direction readings from all the sonic sensors tested are comparable to the original direction calibration setting for the individual sensors.

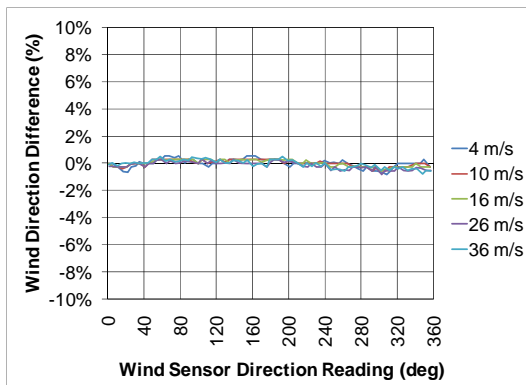


Figure 7: Percent wind DIRECTION difference for the Gill WindObserver II.

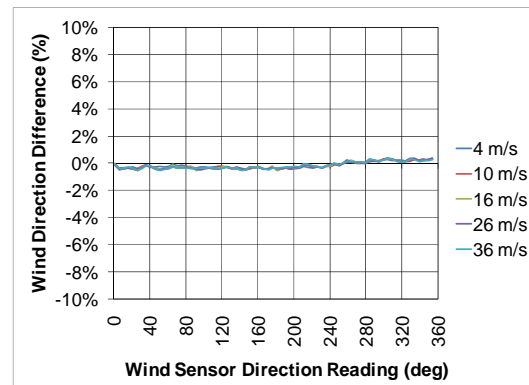


Figure 9: Percent wind DIRECTION difference for the Met One 50.5.

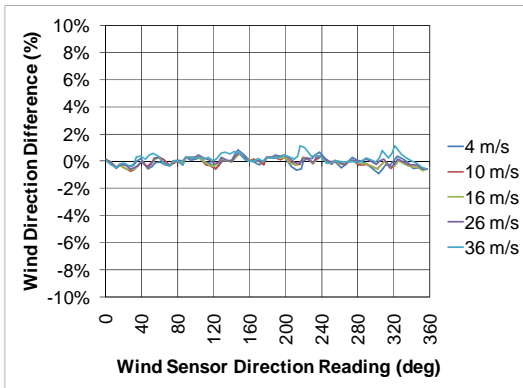


Figure 8: Percent wind *DIRECTION* difference for the Gill WindSonic.

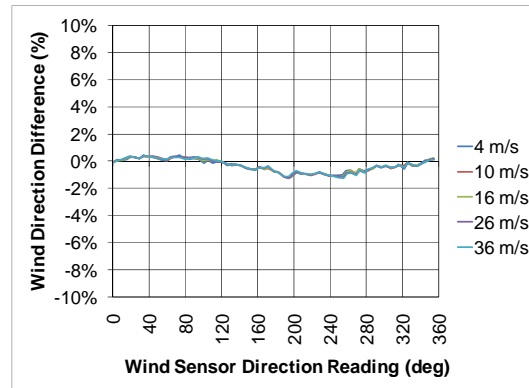


Figure 10: Percent wind *DIRECTION* difference for the R.M. Young 85000.

Wind speed differences between the reference wind tunnel speed and the sonic sensor wind speed are plotted in the following Figures 11 to 14. As expected, these measurements indicated that the highest deviations in sonic sensor wind speeds mainly occurred at positions near 0, 90, 180, and 270 degrees, where the sonic readings were disturbed by an upwind transducer. The smallest deviations in wind speed readings were found near 45, 135, 225, and 315 degrees, which least disturbed by an upwind obstruction. An opposite result was found only with the R.M. Young 85000 since its angle orientation settings having direct upwind disturbance are set 45 degrees offset from the other sonic sensors.

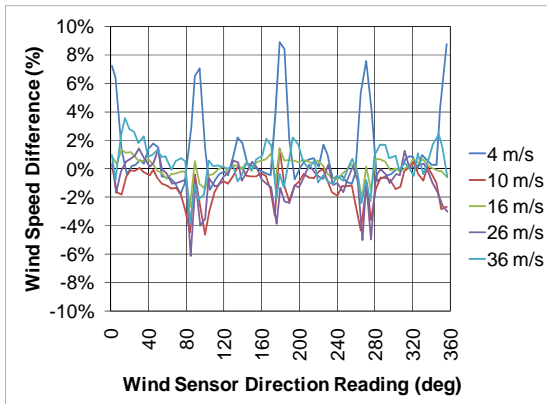


Figure 11: Percent wind *SPEED* difference for the Gill WindObserver II.

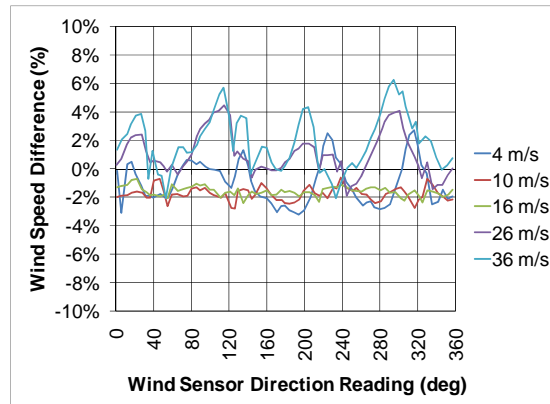


Figure 12: Percent wind *SPEED* difference for the Gill WindSonic.

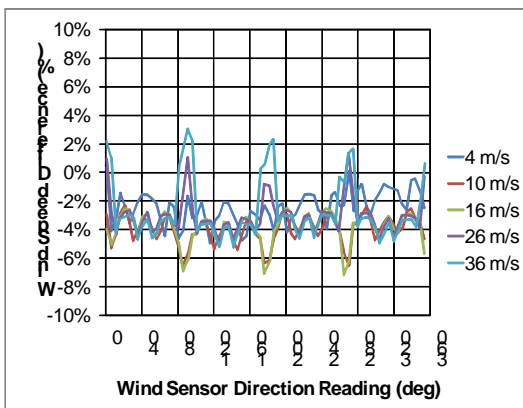


Figure 13: Percent wind *SPEED* difference for the Met One 50.5.

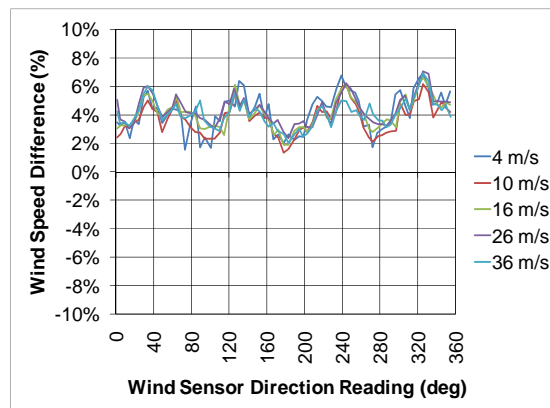


Figure 14: Percent wind *SPEED* difference for the R.M. Young 85000.

According to the overall expanded uncertainty analysis in the wind speed readings from Direction Tests performed for each sonic sensor tested shown in Figure 15, the reference wind speed and sonic sensor speed uncertainty (blue and red columns, respectively) revealed the lowest contributions of errors in the test. Most of the errors were dominated by the standard deviation in the wind speed differences (light blue column) over the entire range of rotations, and even more from the average wind speed difference (green column) from all direction orientations. The overall expanded uncertainty is shown in the lavender column.

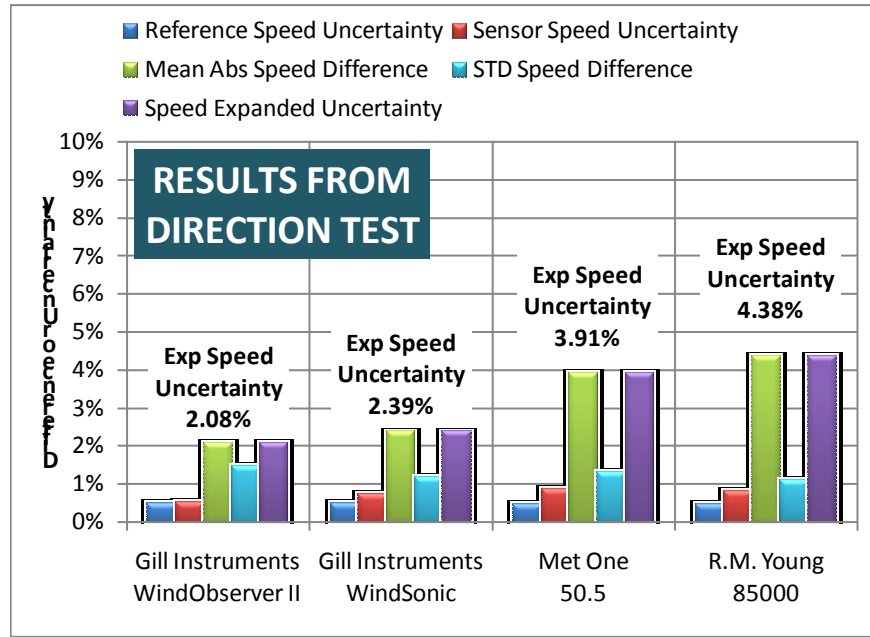


Figure 15: Overall expanded uncertainty from the sonic sensor Direction Tests.

G. Results from Verification Tests

From the Direction Tests, it was found that the similar wind speed differences generally occurred at positions near 0, 90, 180, and 270 degrees for the Gill WindObserver II, Gill WindSonic, and Met One 50.5 sensors. Another set of high wind speed differences were also found near 45, 135, 225, and 315 degrees for the R.M. Young 85000. Thus, as a balance for the study, Verification Tests were performed at the two direction orientations of 135 and 180 degrees. Verification Tests are essentially similar to a calibration test where the sensor output is related to a set of traceable reference wind speeds. Figures 16 to 19, as follows, display the time plots of the reference wind speed and sensor speed readings during a Verification Test. Here, comparisons were only made at the levels of constant wind speed.

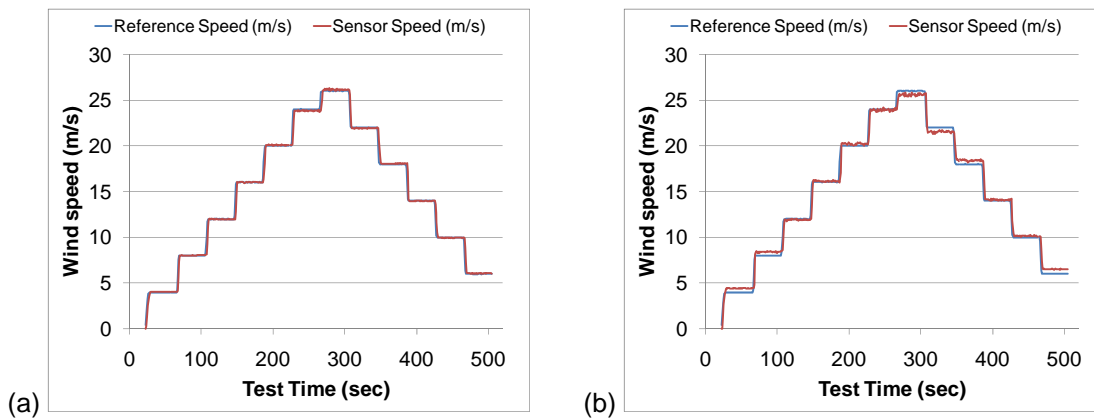


Figure 16: Verification Test at (a) 135 degree and (b) 180 degree orientation of the Gill WindObserver II.

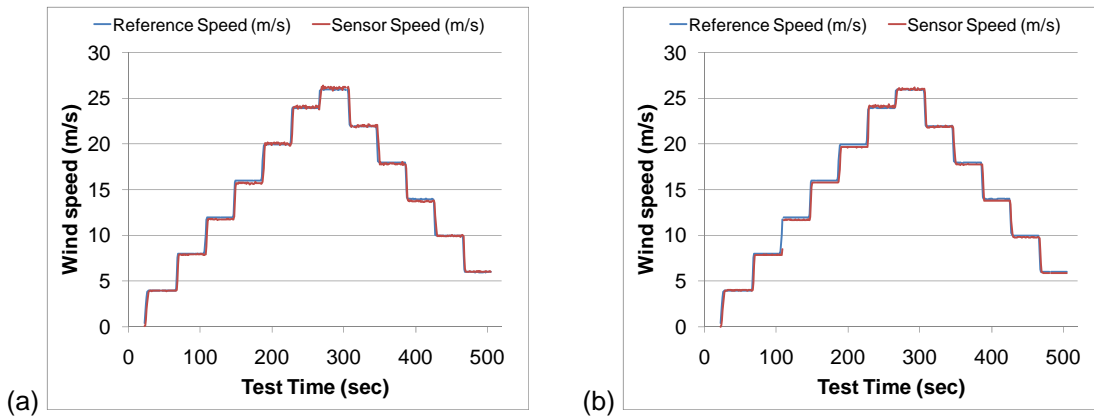


Figure 17: Verification Test at (a) 135 degree and (b) 180 degree orientation of the Gill WindSonic.

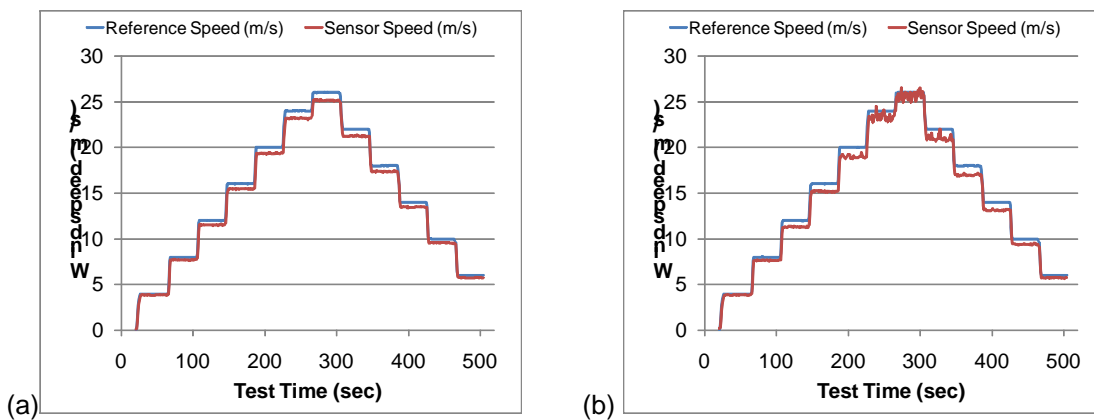


Figure 18: Verification Test at (a) 135 degree and (b) 180 degree orientation of the Met One 50.5.

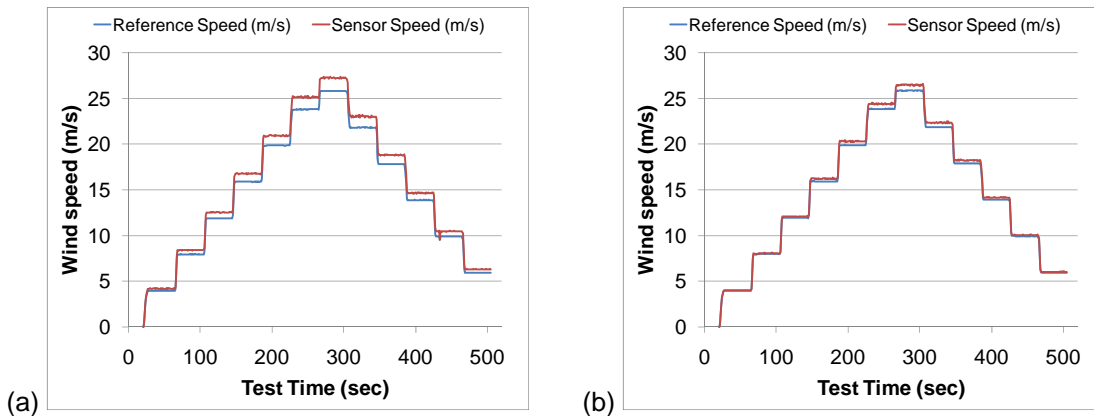


Figure 19: Verification Test at (a) 135 degree and (b) 180 degree orientation of the R.M. Young 85000.

Verification Test time plots of the Gill WindObserver II (Figure 16b) and the R.M. Young 85000 (Figure 19b) show slight deviations between the reference wind speed and the sensor wind speed for the 180 degree orientations. Greater deviations are evident in the 135 and 180 degree orientations of the Met One 50.5 sonic sensor (Figure 18a and 18b) and in the 135 degree orientation of the R.M. Young 8500 (Figure 19a). The following Figure 20 shows the average wind speed differences determined at the 135 and 180 degree orientations of the Verification Tests. Here, the Met One 50.5 at 180 degrees orientation showed a high deviation in wind speed reading from the reference wind speed, while a slightly higher deviation appeared with the R.M. Young 85000 at the 135 degree orientation. These deviations would later show as a major contributor to the overall expanded uncertainty.

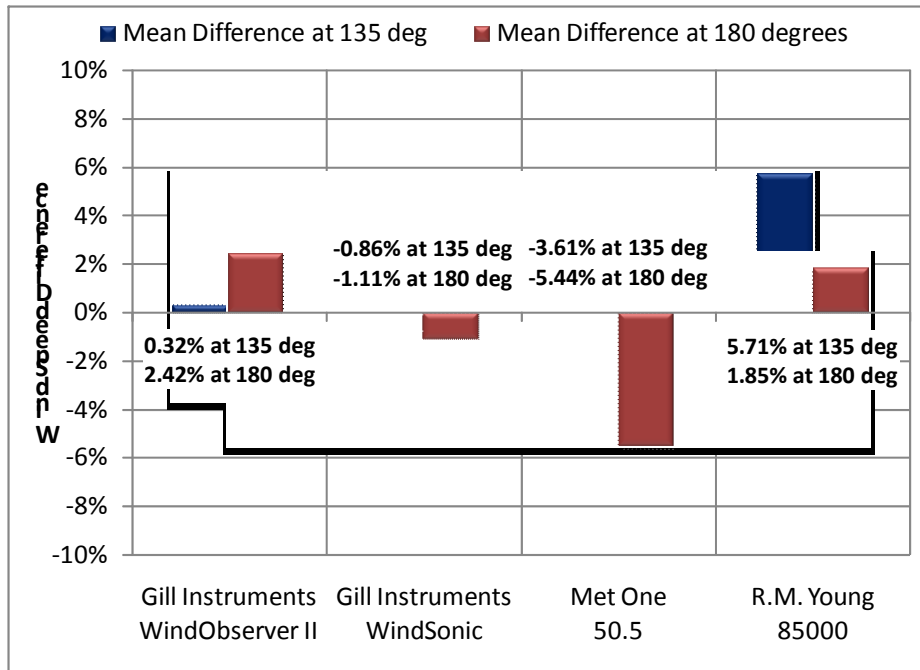


Figure 20: Wind speed differences from Verification Tests.

According to Figure 18b, the Met One 50.5 also showed a greater variability in the sensor output at the higher test speeds of the 180 degree orientation. This variability also increased the uncertainty in the sensor output from the Met One 50.5. The following Figure 21 shows the overall sonic sensor uncertainty from the Verification Tests. From the uncertainty procedures detailed in Part E of this paper, sonic sensor uncertainty is represented by the standard deviation of the sonic sensor reading at a steady wind tunnel speed. As evident from the time plots and shown in Figure 21, the variability of the Met One 50.5 at the higher wind speed settings in the 180 degree orientation resulted in an average sonic sensor uncertainty of 1.68%, nearly double of that of the Gill WindObserver II.

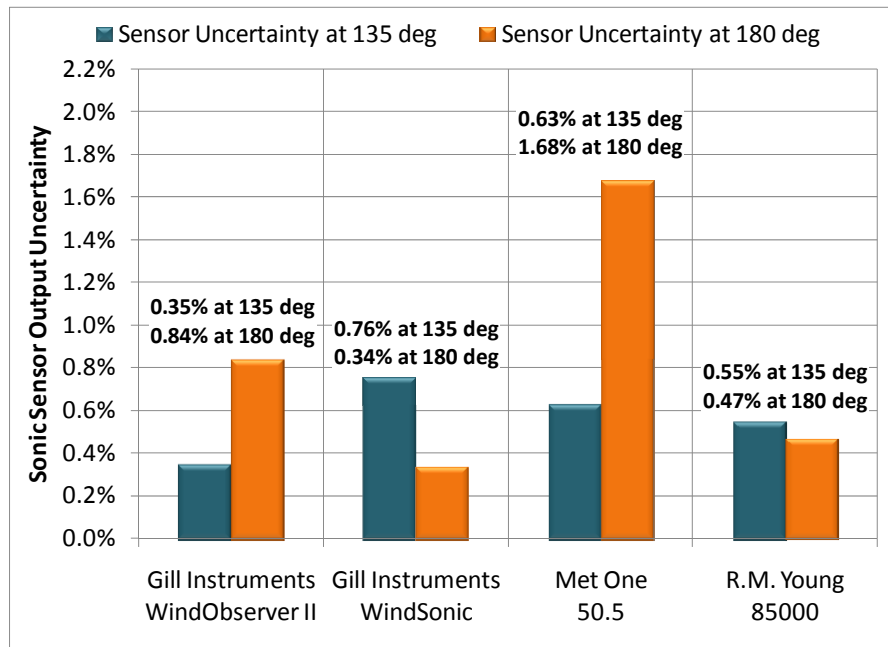


Figure 21: Overall sonic sensor uncertainty from Verification Tests.

Figure 22, as follows, shows a summary of the overall expanded uncertainty in the wind speed readings from the Verification Tests. Here, the reference wind speed uncertainty and sonic sensor speed uncertainty showed the lowest contributions of errors in the tests, consistent with the findings of similar uncertainties from the Direction Tests. In comparison to the Direction Tests, test uncertainties were also dominated by the standard deviation in the wind speed differences over the entire range of rotations, and even more so from the average wind speed difference from all direction orientations. Since test procedures were performed in the orientations indicating the most and least disturbed sonic sensor wind speed readings, the Verification Test provides a conservative view of the overall performance of the sensor when subjected to only horizontal flow. The trends in the values of expanded speed uncertainty in the Verification Tests are also comparable to those determined from the more extensive Direction Tests.

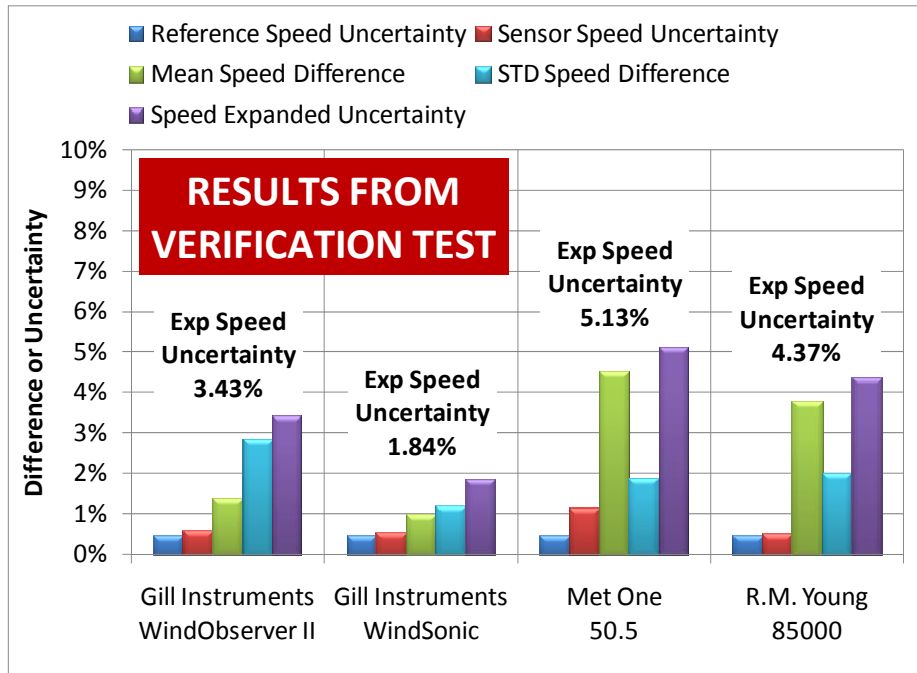


Figure 22: Overall expanded uncertainty from the sonic sensor Verification Tests.

H. Conclusion

Due to the three-dimensional sensitivity of sonic sensors, test standards involve several test setups that would capture the overall performance of these types of sensors. The purpose of this project is to propose a sonic sensor verification protocol that is extracted from test standards, but yet generally identify the uncertainties in a sonic sensor reading. This project presented two types of test methods to determine the overall verification performance of a sonic sensor: 1) Direction Test and 2) Verification Test. The Direction Test is the more rigorous method, where measurements from the sonic sensor are collected for direction orientations at each 5 degree increment around a 360 degree rotation of the sensor. This method identified the direction orientations at which the sonic sensor readings are most and least disturbed. The Verification Test, on the other hand, requires wind speed measurements at only two direction orientations. Based on the findings from the Direction Tests, the Verification Test measurements were done at one orientation with the most disturbed sensor readings and at another where the sonic sensor is least disturbed. A Verification Test is essentially similar to a calibration test in that the sensor output is related to a range of reference wind speeds. As shown in the following Table 3, an overall expanded uncertainty analysis showed comparable values between the more extensive Direction Test and the Verification Test methods. Thus, the less rigorous, yet more strategic Verification Test method may provide a conservative representation of the sonic sensor performance.

Table 3: Comparison of overall uncertainties determined from the Direction Tests and Verification Tests.

<i>Sonic Sensor Model</i>	<i>Direction Test Overall Uncertainty</i>	<i>Verification Test Overall Uncertainty</i>
Gill WindObserver II	2.08%	3.43%
Gill WindSonic	2.39%	1.84%
Met One 50.5	3.91%	5.13%
R.M. Young 85000	4.38%	4.37%

I. Future Work Considerations

Since this paper presents a preliminary proposal of test methods, further study is necessary in the details of the test facility requirements, test procedures, and in the analysis methods. One critical area regarding facility requirements is the effect of model blockage in a wind tunnel test section. This project showed an evaluation of the blockage based on the area ratios of the sensor frontal area and the test section cross-sectional area. However, blockage correction to the test data was not applied due to a need of further understanding the resulting complex three-dimensional flow generated from the sonic sensor body. Another area of further study is in the expanded uncertainty analysis. This study showed that the overall test uncertainty was based on the propagation of errors from all measurements in the wind tunnel including that from the sonic sensor under test. More investigation is required in the uncertainty due to the relationship of the sonic sensor output to the reference wind tunnel speed. Here, this was determined based on wind speed differences, which may generally define the bias between the test facility that offered the sonic sensor's original calibration and the test facility in which verification testing is done.

References

- (1) ASTM D 6011-96 (2008). Standard test method for determining the performance of a sonic anemometer/thermometer. American Society for Testing and Materials.
- (2) IEC 61400-12-1 1st ed 2005-12 (2005). Wind turbines – Part 12-1: Power performance measurements of electricity producing wind turbines. International Electrotechnical Committee.
- (3) ISO 16622 (2002). Meteorology – Sonic anemometers/thermometers – Acceptance test methods for mean wind measurements. International Organization for Standardization.
- (4) ISO/IEC 17025 (2005). General requirements for the competence of testing and calibration laboratories. International Organization for Standardization and International Electrotechnical Committee.
- (5) ISO/IEC Guide 98-3 (2008). Uncertainty of Measurement Part 3: Guide to the Expression of Uncertainty in Measurement (GUM:1995). International Organization for Standardization and International Electrotechnical Committee.
- (6) Coleman, H.W. and W.G. Steele, Jr. (2009). *Experimentation and Uncertainty Analysis for Engineers*, 3rd ed. John Wiley & Sons, Inc, New York, NY.